Cell Stem Cell
Article

Secretion of Shh by a Neurovascular Bundle Niche Supports Mesenchymal Stem Cell Homeostasis in the Adult Mouse Incisor

Hu Zhao,[1] Jifan Feng,[1] Kerstin Seidel,[2] Songtao Shi,[1] Ophir Klein,[2] Paul Sharpe,[3] and Yang Chai[1,*]
[1]Center for Craniofacial Molecular Biology, Ostrow School of Dentistry, University of Southern California, 2250 Alcazar Street, Los Angeles, CA 90033, USA
[2]Department of Orofacial Sciences and Pediatrics, University of California, San Francisco, 513 Parnassus Avenue, San Francisco, CA 94143, USA
[3]Department of Craniofacial Development and Stem Cell Biology, Dental Institute, Kings College London, London TN3 9TF, UK
*Correspondence: ychai@usc.edu
http://dx.doi.org/10.1016/j.stem.2013.12.013

SUMMARY

Mesenchymal stem cells (MSCs) are typically defined by their in vitro characteristics, and as a consequence the in vivo identity of MSCs and their niches are poorly understood. To address this issue, we used lineage tracing in a mouse incisor model and identified the neurovascular bundle (NVB) as an MSC niche. We found that NVB sensory nerves secrete Shh protein, which activates Gli1 expression in periarterial cells that contribute to all mesenchymal derivatives. These periarterial cells do not express classical MSC markers used to define MSCs in vitro. In contrast, NG2$^+$ pericytes represent an MSC subpopulation derived from Gli1+ cells; they express classical MSC markers and contribute little to homeostasis but are actively involved in injury repair. Likewise, incisor Gli1$^+$ cells, but not NG2$^+$ cells, exhibit typical MSC characteristics in vitro. Collectively, we demonstrate that MSCs originate from periarterial cells and are regulated by Shh secretion from an NVB.

INTRODUCTION

Mesenchymal stem cells (MSCs) were first identified in the bone marrow as a group of colony-forming cells with osteogenic, chondrogenic, and adipogenic potential (Friedenstein et al., 1968). MSCs have since been identified from various tissues, including skeletal muscle (Dellavalle et al., 2011), adipose tissue (Tang et al., 2008; Zuk et al., 2002), placenta (Covas et al., 2008), endometrium (Schwab and Gargett, 2007), deciduous teeth (Miura et al., 2003), and bone (Pittenger et al., 1999). Similarities between MSCs and perivascular cells have been characterized, suggesting that they may represent the same population, at least in some tissues (Covas et al., 2008; Schwab and Gargett, 2007). The best-characterized properties of MSCs include their capacity for multipotential differentiation and their immunomodulation abilities (Bernardo and Fibbe, 2013). MSCs are able to differentiate into various cell types in vitro, including osteoblasts, chondrocytes, adipocytes, or even neurons (Keating, 2012). Although MSCs have been extensively studied, their in vivo identity and supporting niche remain elusive. The definition of MSCs is based on a loose set of criteria including trilineage in vitro differentiation ability and expression of various MSC surface markers (Bianco et al., 2013; Dominici et al., 2006; Keating, 2012). To date, there are no well-defined in vivo markers or appropriate lineage analysis tools for MSCs. Similarly, although label-retaining or lineage-tracing analyses have become the gold standard for many other stem cell studies (Grompe, 2012), these techniques have rarely been applied to MSC studies (Méndez-Ferrer et al., 2010; Tang et al., 2008). Thus, at present, MSCs are defined based on their in vitro culture properties and expression profiles of multiple surface markers, with considerable controversy (Bianco et al., 2013; Keating, 2012). Based mostly on these criteria, it was proposed that the perivascular niche is an in vivo niche of MSCs and that pericytes are their in situ counterparts (Covas et al., 2008; Crisan et al., 2008; Traktuev et al., 2008). However, rigorous testing is necessary to evaluate this theory and to determine whether other sources may provide an MSC niche.

The mouse incisor provides an excellent model for MSC study because it grows continuously throughout the life of the animal. It is composed of an outer enamel surface, dentin underneath the enamel, and dental pulp in the center containing vasculature and nervous tissue. Both epithelial and mesenchymal compartments of the incisor rapidly replenish all of their cells within 1 month (Smith and Warshawsky, 1975). Self-renewal of the incisor epithelium is supported by a group of quiescent epithelial stem cells in the cervical loop region (Juuri et al., 2012; Seidel et al., 2010). Although incisor dentin is highly similar to bone, two properties that make the incisor unique from bone are its well-oriented structures and fast turnover. The odontoblasts, which form dentin, are aligned in a single layer along the inner surface of the dentin, and their arrangement displays a cytodifferentiation gradient from the immature region apically toward the tip. The vasculature and nerves of the incisor are well organized and oriented in one direction. The continuous turnover of odontoblasts is supported by stem cells within the mesenchyme, but the identity and exact localization of these stem cells in vivo remains unknown (Balic and Mina, 2010; Mao and Prockop,

2012). It has been proposed that incisor MSCs are localized near the cervical loop region that can give rise to transit amplifying cells (TACs) (Feng et al., 2011; Lapthanasupkul et al., 2012). TACs can be easily identified based on their active proliferation, and they give rise to committed preodontoblasts and then terminal differentiated odontoblasts. This rapid turnover makes the incisor mesenchyme an excellent model for studying MSCs.

The role of nerves in the regulation of the stem cell niche remains largely unknown. The sensory nerves innervating the hair follicle regulate the response of a group of hair follicle stem cells during injury repair (Brownell et al., 2011). Sympathetic innervation regulates hematopoietic stem cell egression from the bone marrow (Katayama et al., 2006) and their emergence during embryogenesis (Fitch et al., 2012). Adrenergic nerves associate with and regulate nestin$^+$ bone marrow MSCs (Méndez-Ferrer et al., 2010). Parasympathetic nerves are essential for epithelial progenitor cells during salivary gland organogenesis and for adult gland injury repair (Knox et al., 2010, 2013). In adult tissues, nerves travel along the arteries. Together with the loose connective tissue surrounding arteries and nerves, they form a neurovascular bundle (NVB), which is a common anatomical structure found in many organs.

In this study, we use the mouse incisor as a model to determine the in vivo identity of MSCs and their corresponding niche. We show that incisor MSCs surround the arterioles and are supported by an NVB niche. These periarterial MSCs participate in both homeostasis and injury repair of incisor mesenchyme in vivo and give rise to the entire MSC population in vitro.

RESULTS

Label-Retaining Cells Surround the NVB

In the mouse incisor, major arteries and veins are arranged in parallel along the long axis with the arterial branches aligned on the midline bisecting the incisor (Figure S1 available online). Nerves in the incisor accompany arteries to form the NVB (Figure S1). To investigate the in vivo mechanism of MSC-supported incisor mesenchyme homeostasis, we performed label-retaining analysis. H2BGFP-based label-retaining analysis has been used for identifying stem cells in various tissues (Foudi et al., 2009; Tang et al., 2008; Tumbar et al., 2004). We generated triple-transgenic mice, *Wnt1-Cre;ROSA26$^{LoxP\text{-}STOP\text{-}LoxP\text{-}tTA}$; tetO-H2BGFP* (WTH) (Figure S2A), to identify label-retaining cells (LRCs) in the dental mesenchyme. After confirming that doxycycline exerts stringent control over H2BGFP expression in the dental mesenchyme (Figure S2B), we performed label-retaining analysis using 4- to 6-week-old WTH mice followed by a 4-week chase period. Our experimental design was based on a time course study (Figures S2D–S2I) and the previous finding that odontoblasts and ameloblasts in mouse incisors are turned over within 1 month (Harada et al., 1999; Smith and Warshawsky, 1975). After complete H2BGFP labeling of the dental pulp and a 4-week chase, all LRCs surround the NVB, centered on arteries and accompanying nerves, but not on veins or capillaries. (Figures 1A–1C). The dental mesenchyme near the cervical loop contains fast-dividing TACs (Lapthanasupkul et al., 2012; Parsa et al., 2010). Short-term 5-ethynyl-2′-deoxyuridine (EdU) incorporation experiments indicate that LRCs and EdU-positive TACs are adjacent to, but mutually exclusive from, each other, with LRCs near the NVB in the center surrounded by TACs (Figures 1D and 1E). Next, we injured incisors with a needle and collected samples 24 hr later. EdU was injected 2 hr before sacrifice. In injured incisors, approximately 10% of H2BGFP LRCs incorporated EdU, indicating that the normally slow-cycling mesenchymal cells (LRCs) were stimulated by injury to proliferate (Figures 1F–1H).

Gli1$^+$ Cells Surrounding the NVB Are MSCs Supporting the Homeostasis and Injury Repair of Incisor Mesenchyme

Previous results have suggested that Gli1 may be a dental epithelial stem cell marker (Seidel et al., 2010). We hypothesized that Gli1 might also be a marker for incisor MSCs. We analyzed the Gli1 expression pattern in incisors using *Gli1-LacZ* mice. We detected Gli1 expression in the mesenchyme surrounding the NVB, centered on arteries and accompanying nerves, but not veins or capillaries (Figures 2A–2C). Gli1 expression was also detectable in dental epithelial cells (Figure 2A) and in the postmitotic odontoblasts of the labial side mesenchyme. A similar Gli1$^+$ expression pattern in the incisor was also detectable in Gli1-GFP mice (Figure S3A). Fluorescence-activated cell sorting (FACS) analysis of incisors from Gli1-GFP mice indicated that there are around 2,300 Gli1$^+$ cells in each lower incisor, comprising less than 5% of the entire incisor mesenchyme population (Figure S3B). To determine whether Gli1$^+$ cells support incisor homeostasis, we generated *Gli1-Cre^{ERT2}*; *ROSA26$^{LoxP\text{-}STOP\text{-}LoxP\text{-}ZsGreen1}$* (*Gli1-CE;Zsgreen*) mice and injected tamoxifen at 4–6 weeks of age. We detected ZsGreen$^+$ cells near the cervical loop region 72 hr after the first injection (Figure 2D). This ZsGreen$^+$ population included Gli1-expressing cells and the derivatives they produced within the last 72 hr. Over a 4-week period, Gli1$^+$ cells expanded toward the tip of the incisor and eventually populated the entire dental mesenchyme (Figure 2D). To test whether Gli1$^+$ cells can self-renew and continuously support mesenchyme turnover, we examined Gli1 expression at 6 months of age (Figure S3H). In *Gli1-CE; ZsGreen* mice induced at 6 months, a small number of ZsGreen$^+$ cells were detectable in the cervical loop region 72 hr after the first injection and after 1 month the entire pulp mesenchyme was populated by Gli1$^+$ cell derivatives (Figures S3I and S3J). Moreover, we assessed *Gli1-CE;ZsGreen* incisor samples at 4 and 17.5 months after induction and found that the entire mesenchyme was still populated with Gli1$^+$ cell derivatives (Figures S3C and S3D).

To compare the LRC and Gli1$^+$ populations, we generated *Gli1-LacZ;WTH* tetra-transgenic mice in which LRCs are labeled with H2BGFP and Gli1$^+$ cells are labeled with β-galactosidase (β-gal). Colocalization of β-gal and LRC signals indicate that around 95% ± 0.06% of Gli1$^+$ cells are quiescent LRCs and 80% ± 0.09% of LRCs are Gli1$^+$, suggesting heterogeneity of both the Gli1$^+$ and LRC populations (Figures 2E and 2F). Similar to LRCs, Gli1$^+$ cells and TACs are adjacent to but mutually exclusive from each other, further supporting our conclusion that Gli1$^+$ cells are MSCs in the incisor mesenchyme (Figure 2G).

To test whether Gli1$^+$ cells can be activated upon injury, we injured incisors of 1-month-old *Gli1-LacZ* mice. Gli1 activity was not significantly changed 48 hr after injury (Figure S3E). EdU incorporation experiments indicate that Gli1$^+$ cells begin

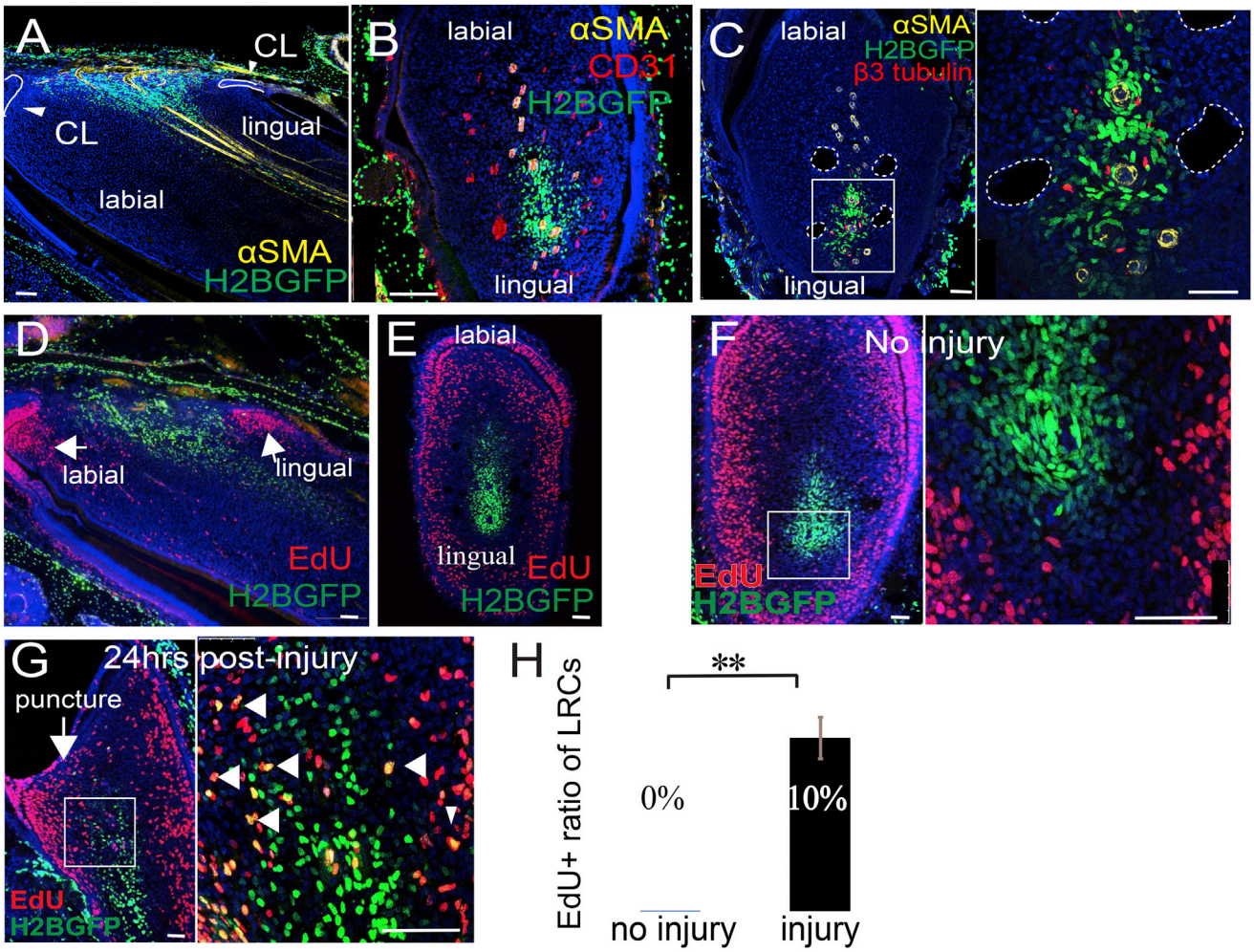

Figure 1. The Neurovascular Bundle Provides a Niche for Quiescent Stem Cells

(A and B) Sagittal (A) and cross sections (B) of *WTH* mouse incisors chased for 1 month (LRCs appear green due to H2BGFP), after αSMA (yellow) and CD31 (red) immunohistochemical staining. In the sagittal sections, the apical region of the incisor is oriented to the left side. In the cross sections, the labial side of the incisor is oriented to the top. αSMA labels arteries. CD31 labels all vasculature. CL, cervical loop.

(C) β3-tubulin (red) and αSMA (yellow) staining of cross sections of chased *WTH* mouse incisors. β3-tubulin labels nerves. Boxed area is shown magnified to the right. Dotted white lines outline veins.

(D and E) Sagittal (D) and cross (E) sections of chased adult *WTH* mouse incisors treated with EdU (red).

(F and G) Chased *WTH* mouse incisors treated with EdU (red) without (F) or with (G) injury to the tooth. Arrow indicates injury site (puncture). Arrowheads indicate double labeling (yellow) of LRCs and EdU incorporation. Boxed areas are shown magnified to the right. Nuclear DAPI staining is in blue.

(H) Quantification of LRCs incorporating EdU before and after injury, as shown in (F) and (G). Values are plotted as mean ± SEM (n = 5, at least 500 cells were counted in each sample; $^{**}p < 0.01$. n = 4).

Scale bars, 100 μm.

proliferating by 24 hr after injury (Figure S3F). To determine whether Gli1$^+$ cells can contribute to injury repair, we first induced 1-month-old *Gli1-CE;ZsGreen* mice with tamoxifen and then injured the incisor 72 hr after induction. Two weeks after injury, reparative dentin had formed, as indicated by the distorted shape and disorganized dentin tubules (Figure 2H, asterisk), and was derived from Gli1$^+$ cells (Figure 2I). Therefore, Gli1$^+$ cells in the incisor are quiescent MSCs that support both homeostasis and injury repair.

Gli1 is a member of the hedgehog signaling pathway that responds to hedgehog family ligands (Jiang and Hui, 2008). To determine the role of the hedgehog pathway in regulating incisor MSCs, we fed adult mice Shh inhibitor HhAntag for 1 month as previously described (Seidel et al., 2010). Inhibitor administration significantly reduced Gli1 activity in the incisor (Figures S3K and S3L). Treatment with inhibitor also significantly reduced dentin formation but had little effect on cell proliferation within the mesenchyme (Figures S3M–S3P). The administration of inhibitor had no significant effect on mesenchymal cell apoptosis or the number of LRCs within the incisor mesenchyme, suggesting that stem cell maintenance was not affected (Figures S2Q–S2U). In addition, we tested the effect of Shh on incisor MSCs in vitro. Shh at various concentrations had no significant effect on cell proliferation (Figure S3V). Alizarin red staining and

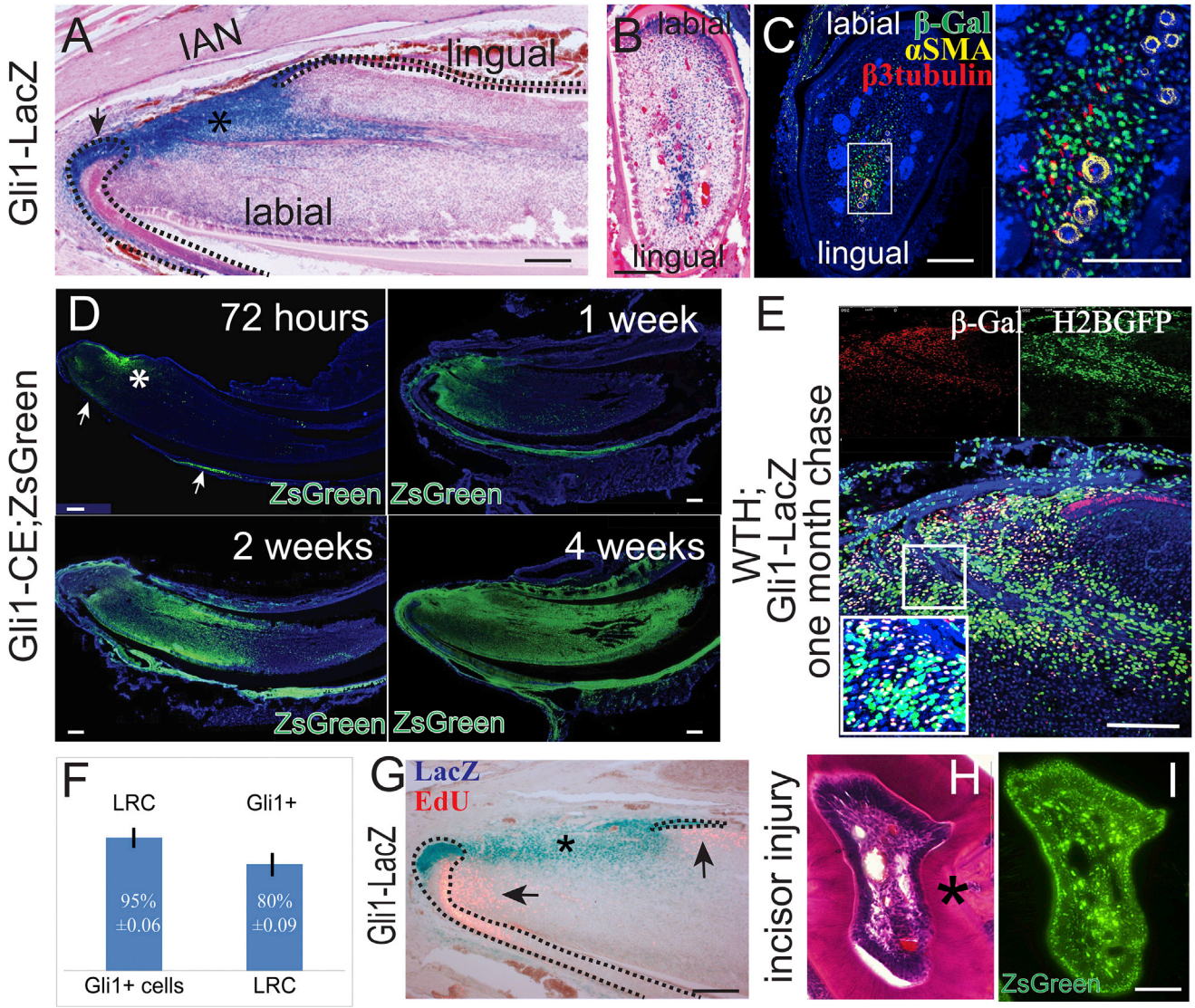

Figure 2. Gli1$^+$ Cells Surrounding the Neurovascular Bundle Support Tissue Homeostasis and Injury Repair

(A–C) LacZ staining (blue) of sagittal (A) and cross (B) sections; β-gal (green), αSMA (yellow), β3-tubulin (red), and DAPI (blue) immunohistochemical staining of adult *Gli1-lacZ* incisor (C). αSMA and β3-tubulin label arteries and nerves, respectively. Boxed area in (C) is shown magnified to the right. Asterisk indicates Gli1 activity in the mesenchyme. Arrow indicates Gli1 activity in the epithelium. Dotted lines outline cervical loop dental epithelium.

(D) Time course of Gli1$^+$ cell lineage tracing (green) in adult *Gli1-CE;ZsGreen^{flox}* mice after tamoxifen induction. Asterisk indicates incisor mesenchyme derived from Gli1$^+$ cells. Arrows indicate Gli$^+$ cell derivatives in the epithelium.

(E) β-gal staining in chased adult *WTH;Gli1-LacZ* tetra-transgenic mouse incisors shows Gli1$^+$ and LRC colocalization. Red β-gal staining indicates Gli1 expression. LRCs appear green from H2BGFP. The boxed area is enlarged in the inset. Yellow cells are double stained for Gli1$^+$/LRCs.

(F) Quantification of results from (E). 95% ± 0.06% of Gli1$^+$ cells are LRCs, whereas 80% ± 0.09% of LRCs are Gli1$^+$. Values are plotted as mean ± SEM (n = 4).

(G) LacZ (blue) and EdU (pink) staining of incisors from 6-week-old *Gli1-LacZ* mice. EdU was injected 2 hr before collecting samples. Dotted lines outline cervical loop dental epithelium.

(H–I) H&E staining (H) and fluorescent image (I) of incisor cross sections from 4- to 6-week-old *Gli1-CE;ZsGreen* mice after incisor injury. Asterisk indicates reparative dentin formation. Images from adjacent sections show the contribution of Gli1$^+$ cells to reparative dentin formation.

Scale bars, 100 μm.

real-time PCR indicated that odontogenic differentiation was enhanced by the presence of Shh (Figures S3W and S3X). Based on both in vivo and in vitro data, we conclude that Shh in the incisor mainly functions to regulate the odontogenic differentiation process but has little effect on stem cell maintenance or cell proliferation.

Sensory Nerves in the Mesenchyme Provide Shh for the Periarterial Gli1$^+$ Cells

A previous report suggested that Shh from the dental epithelium triggers mesenchymal Gli1 activity (Seidel et al., 2010), but this model cannot explain the specific peri-NVB Gli1+ pattern. To test whether dental epithelial Shh signaling activates Gli1 in

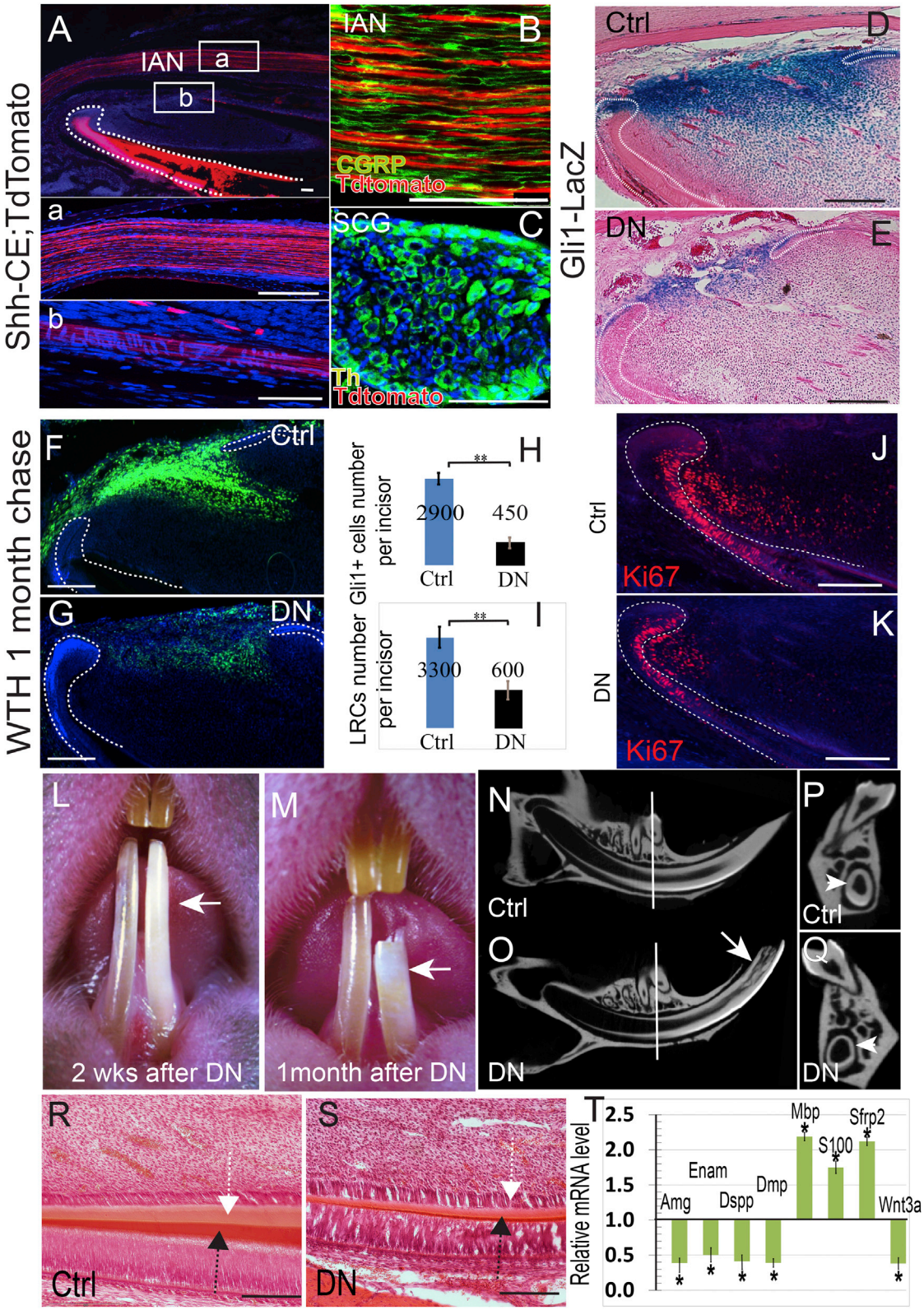

Figure 3. Sensory Nerves Provide Shh to Gli1⁺ Cells

Denervation disrupts the incisor MSC niche and causes abnormal phenotypes.

(A) Adult *Shh-CE;TdTomato* mouse incisors 2 weeks after tamoxifen induction. Boxed areas (a) and (b) are shown magnified below. Note the Shh expression (red) in the inferior alveolar nerve (IAN) (a) and nerve bundles accompanying the artery (b). Dotted lines outline the dental epithelium. DAPI staining is in blue.

(legend continued on next page)

the dental mesenchyme, we generated *K14-rtTA;tetO-Cre; Shh*$^{flox/flox}$ mice (*K;T;Shh*). Doxycycline induction at 1 month of age efficiently eliminated Shh expression in the dental epithelium (Figures S4A, S4B, S4A′, and S4B′). However, no defect was detectable in *K;T;Shh* mutant incisors 1 month after induction. Enamel and dentin mineralization are indistinguishable in *K;T; Shh* and control incisors based on micro-computed tomography (micro-CT) images (Figures S4C and S4D). Proliferation analysis and hematoxylin and eosin (H&E) staining also demonstrated no significant difference between *K;T;Shh* and control incisors (Figures S4E–S4H, S4G′, and S4H′). Most importantly, Gli1 expression surrounding the NVB was not affected in *K;T;Shh* incisors (Figures S4I and S4J). To confirm the specificity of our Gli1 antibody, we also performed immunohistochemical staining using *Gli1*$^{LacZ/LacZ}$ (*Gli1*$^{-/-}$) incisors (Bai et al., 2002), which showed no signal surrounding the NVB (Figure S4K). Therefore, we conclude that Shh derived from the incisor epithelium does not trigger Gli1 activity in the mesenchyme and that Gli1^{+} cells must be supplied by a different Shh source.

To identify other Shh sources, we generated *Shh-Cre*^{ERT2}*; ROSA26*$^{LoxP\text{-}STOP\text{-}LoxP\text{-}TdTomato}$ (*Shh-CE;Tdtomato*) mice in which Shh-producing structures can be labeled by TdTomato fluorescence upon induction. Three days after the first tamoxifen injection, strong Shh activity was detectable in the trigeminal ganglion (TGG) (Figure S5A), which contains most of the neuron bodies innervating the craniofacial region. Immunohistochemical staining with the sensory nerve marker calcitonin gene-related peptide (CGRP) indicated these Shh-secreting neurons are sensory neurons. Strong Shh activity was also detectable in the incisor epithelium, but not in any mesenchymal cells, 3 days after induction. Two weeks after induction, we detected strong reporter activity in axons of the inferior alveolar nerve (IAN), which is the sole sensory nerve innervating the adult lower incisor (Figures 3A and 3B). The discrepancy between TGG and IAN reporter activity appearance time suggests the TdTomato protein is first synthesized in the TGG sensory neuron cell bodies and then transported along the IAN axons to the incisor mesenchyme. The incisor is also innervated by sympathetic nerves derived from the superior cervical ganglion (SCG) (Ladizesky et al., 2001). We dissected the SCG from induced *Shh-CE; Tdtomato* mice (Savastano et al., 2010) and found no Shh activity, indicating that sympathetic neurons do not produce Shh (Figure 3C). We also conducted Shh immunohistochemical staining in the incisor, which confirmed the presence of Shh protein in the dental epithelium and mesenchyme surrounding nerve fibers in the cervical loop region (Figures S5C, S5C′, and S5C″). Shh protein was also present in the TGG and IAN (Figures S5D and S5E).

To test whether neural Shh is the source for mesenchymal Gli1 activity, we severed the IAN in adult *Gli1-LacZ* mice. Denervation had no effect on incisor circulation or odontoblast morphology (Figures S5G–S5J). No odontoblast degeneration was observed 72 hr after denervation, whereas vascular damage rapidly led to extensive odontoblast degeneration (Figure S5K). To confirm that the nerves were completely removed, we conducted immunohistochemical staining of incisors 1 month after surgery and failed to detect any nerve fibers in the mesenchyme (Figures S5L and S5M). One week after denervation, Shh expression was significantly reduced in the mesenchyme, but not the epithelium (Figure S5F). Gli1 activity in the mesenchyme of the denervated incisor was also significantly reduced (Figures 3D, 3E, and 3H). Interestingly, Gli1 activity in the epithelium was also reduced after denervation (n = 10) (Figure 2E). The number of LRCs was significantly reduced 1 month after denervation (Figures 3F, 3G, and 3I). Denervation reduced the number of proliferating cells in the incisor mesenchyme as well (Figures 3J and 3K), consistent with previous studies (Chiego et al., 1981). Denervated incisors turned chalky about 2–3 weeks after denervation (20/20), and many of the denervated incisors fractured 1 month after the procedure (14/20) (Figures 3L and 3M). Micro-CT analysis and H&E staining indicated reduced enamel and dentin formation in the denervated incisor (Figures 3N–3S), consistent with previous studies (Chiego et al., 1981, 1983; Kerezoudis et al., 1995; Kubota et al., 1985).

To investigate further, we performed microarray analysis of incisors 2 weeks after denervation (Figures S5S–S5U) and found that denervation led to extensive gene expression changes in the incisor mesenchyme. A total of 105 genes were downregulated and 185 genes were upregulated by over 1.5-fold in denervated incisors. Denervated incisors presented a distinctive transcript profile versus the controls (Figure S5S). We performed real-time PCR to confirm changes in the expression of several candidate genes. Amelogenin (Amg), enamelin (Enam), Dspp, and Dmp, which are involved in enamel and dentin terminal differentiation, were significantly downregulated in denervated incisors, consistent with the observed phenotypes (Figure 3T). Denervation led to downregulation of the Wnt signaling pathway via reduced Wnt3a expression and increased expression of

(B) Sensory nerve marker CGRP staining (green) of the IAN in adult *Shh-CE;TdTomato* mouse incisors.
(C) Th staining (green) of the superior cervical ganglion (SCG) in adult *Shh-CE;TdTomato* mouse incisors. The SCG is negative for Shh activity (red). Th staining labels sympathetic neurons.
(D and E) LacZ staining (blue) of control (Ctrl) or denervated (DN) *Gli1-lacZ* incisors indicates significantly reduced Gli1 activity after denervation. Dotted lines indicate the cervical loop epithelium.
(F and G) LRC (green) of control (Ctrl) or denervated (DN) *WTH* incisors 1 month after chasing. Dotted lines outline the dental epithelium.
(H and I) Quantification of results from (D) and (E) (H) and (F) and (G) (I). Values are plotted as mean ± SEM (**$p < 0.01$; n = 5).
(J and K) Ki67 staining shows fewer proliferating cells in the mesenchyme of denervated incisors (K) as compared with control (sham-operated) incisors (J).
(L and M) Denervated incisors (arrow) turn chalky white 2 weeks after surgery (L; n = 20) and fracture within a month (M; n = 14).
(N and Q) Longitudinal micro-CT images of sham-operated (control) incisor (N) and denervated incisor (O). Arrow indicates the fracture site. Cross sections (P and Q) were sampled at comparable positions, indicated by white lines in (N) and (O). Arrowheads indicate the dentin wall of the incisors.
(R and S) H&E staining of control (Ctrl) and denervated (DN) incisor longitudinal sections after 1 month. Note the reduced thickness of the enamel (black arrow) and dentin (white arrow).
(T) Real-time PCR data of indicated genes in denervated incisors compared to control incisors. Values are plotted as mean ± SEM (*$p < 0.05$; n = 4).
Scale bars, 100 μm.

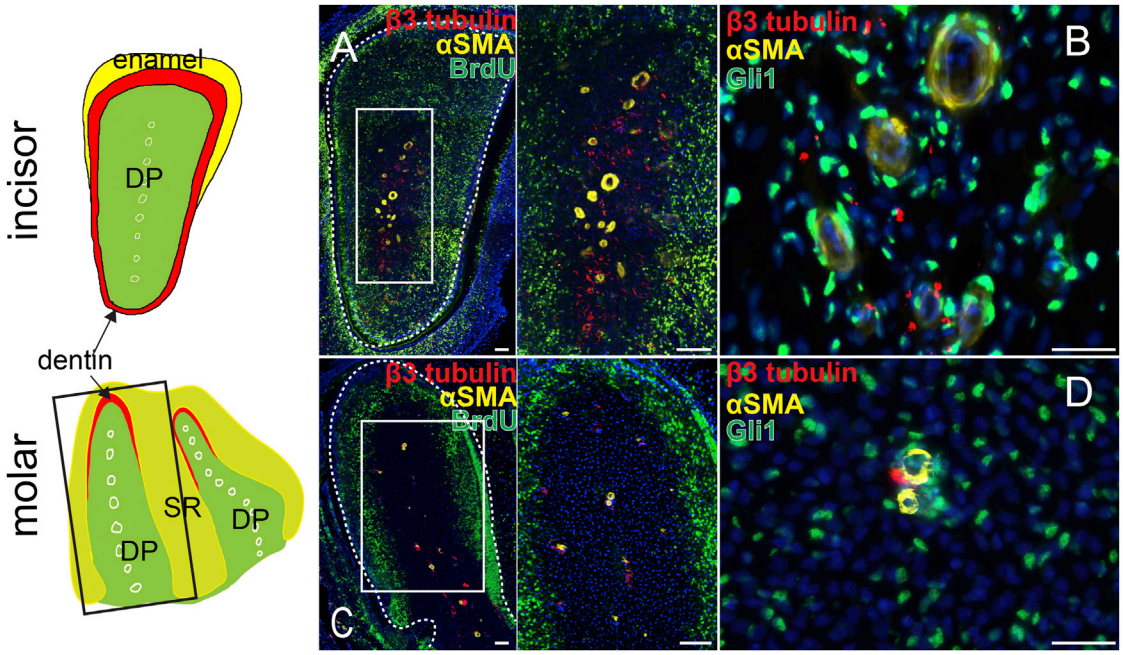

Figure 4. Guinea Pig Molars Contain Quiescent Label-Resisting Cells and Gli1$^+$ Cells Surrounding the Neurovascular Bundle

Schematic drawing depicts a cross section of the anatomy of the guinea pig incisors (top) and a horizontal section of the anatomy of the guinea pig molars (bottom). White circles outline arteries in the dental pulp (DP, green). Box indicates the approximate position of (C). Enamel, yellow. Dentin, red. SR, stellate reticulum (light green).

(A) Cross section of guinea pig incisor injected continuously with BrdU (green) for 10 days and stained with αSMA (yellow) and β3-tubulin (red). Boxed area is shown magnified to the right.

(B) Immunohistochemistry for αSMA (yellow), β3-tubulin (red), and Gli1 (green) in guinea pig incisor.

(C) Horizontal section of guinea pig molar injected continuously with BrdU (green) for 10 days and stained with αSMA (yellow) and β3-tubulin (red). Boxed area is shown magnified to the right.

(D) Immunohistochemistry for αSMA (yellow), β3-tubulin (red), and Gli1 (green) in guinea pig molars. Dotted lines outline dental pulp.

Scale bars, 100 μm.

Wnt signaling inhibitor Sfrp2 (Figure 3T). Wnt inhibition may be related to reduced proliferation in the mesenchyme. Interestingly, myelin basic protein (Mbp) and S100b, which are glial-cell-specific genes, were significantly upregulated upon denervation (Figure 3T), possibly related to the glial cell proliferation following nerve damage (Chen et al., 2007). This result was also confirmed with immunohistochemical staining that showed an increase in glial cells surrounding the arteries 1 month after denervation (Figures S5N and S5O). Denervation had no effect on Gli1$^+$ cell lineage tracing or mesenchymal cell apoptosis (Figures S5P–S5R).

Guinea Pig Molars Contain Quiescent Label-Resisting Cells and Gli1$^+$ Cells Surrounding the NVB

So far, our data strongly suggest that Gli1$^+$ cells surrounding the NVB are quiescent stem cells that support incisor mesenchyme homeostasis and that nerves provide a niche to maintain Gli1$^+$ MSCs. To test this hypothesis further, we examined guinea pigs, which have continuously growing incisors and molars (Hashimoto et al., 2008). In guinea pigs injected with bromodeoxyuridine (BrdU) daily for 10 days, most of the cells in the incisor mesenchyme incorporated BrdU, except for a group of cells surrounding the NVB (Figure 4A), which we named label-resisting cells. These cells must be either quiescent or very active in cell division. Highly active cell division is excluded because the last BrdU injection was given 2 hr before collecting samples. Gli1 expression was also detectable surrounding the incisor NVB (Figure 4B). Similar label-resisting and Gli1$^+$ cells were detectable surrounding the NVB in molars of guinea pigs (Figures 4C and 4D).

Periarterial Gli1$^+$ Cells Do Not Express Classical MSC Markers but Give Rise to NG2$^+$ Pericytes that Express These Markers

Based on our above data, we identified Gli1$^+$ cells as the MSCs that support the homeostasis and injury repair of incisor mesenchyme in vivo. Conventionally, MSCs in vitro are defined based on various surface markers (Bianco et al., 2008; Dominici et al., 2006). Therefore, we conducted surface marker analysis of incisor MSCs. Surprisingly, the majority of LRCs or Gli1$^+$ cells do not express the typical MSC markers CD105 and CD73 or the other MSC-related markers NG2, CD146, CD44, and Sca1 (Figures 5A–5J; Figures S6A–S6C). We also analyzed the expression of nestin, which was previously proposed to be a surface marker for bone marrow MSCs (Méndez-Ferrer et al., 2010). We detected nestin expression in differentiated odontoblasts of the incisors, but not in Gli1$^+$ cells (Figure S6D). CD34 has also been proposed to be a surface marker for a group of

MSCs derived from the tunica adventitia of large arteries (Corselli et al., 2012). We failed to detect expression of CD34 in the incisor (Figure S6E). Most CD44 cells and CD146$^+$ cells are Gli1$^+$ LRCs, but the majority of Gli1$^+$ LRCs are negative for CD44 and CD146 (Figures S6F and S6G).

NG2$^+$ pericytes have been proposed to represent a population of MSCs in the dental mesenchyme (Feng et al., 2011). We examined NG2 expression in the incisor using *NG2-DsRed* mice. NG2$^+$ cells are pericytes immediately surrounding the CD31$^+$ endothelium (Figure 5K). In some tissues, such as gut mesentery, NG2$^+$ cells are distributed preferentially surrounding arterioles (Murfee et al., 2005), but in other tissues, such as retina and brain, they are detectable surrounding all types of vasculature (Chan-Ling and Hughes, 2005; Zhu et al., 2008). We found that NG2$^+$ cells are detectable in the incisor mesenchyme surrounding arterioles, veins, and capillaries (Figure S7D). These NG2$^+$ pericytes express typical MSC markers including CD146, Sca1, and CD105 (Figures 5L–5O). We analyzed the contribution of NG2$^+$ cells to homeostasis using *NG2-Cre;ROSA26$^{LoxP\text{-}STOP\text{-}LoxP\text{-}ZsGreen1}$* (*NG2-Cre;ZsGreen*) mice. In the incisor mesenchyme, NG2$^+$ cells contribute mainly to the vasculature, making little contribution to the pulp mesenchyme or odontoblasts (Figure 5P), as shown in a previous study (Feng et al., 2011). Upon injury, however, the contribution of NG2$^+$ cells to odontoblasts significantly increased (Figures 5Q and 5R).

Based on these results, we investigated the relationship between Gli1$^+$ and NG2$^+$ cells. It is apparent that NG2$^+$ cells do not give rise to all Gli1$^+$ cells (Figure 5P). In contrast, lineage-tracing experiments indicated that Gli1$^+$ cells give rise to the entire incisor mesenchyme except the CD31$^+$ endothelium (Figures 5S and 5T). Specifically, Gli1$^+$ cells give rise to all NG2$^+$ or CD146$^+$ perivascular cells (Figures 5U and 5V).

We also investigated Gli1$^+$ and NG2$^+$ cells in mouse molars. In contrast to incisors, adult mouse molars do not grow continuously. Adult molars do not contain Gli1$^+$ cells (Figure S7A) or LRCs surrounding the arteries (Figures S7B and S7C). NG2$^+$ cells are also found as pericytes surrounding all vasculature in the molars (Figures S7E and S7F) and they express the typical MSC markers CD146, CD105, and Sca1 (Figures S7G–S7J). NG2$^+$ cells contribute mainly to the vasculature of molars with little contribution to odontoblasts in *NG2-Cre;ZsGreen* mice (Figure S7K). Upon injury, NG2$^+$ cells were actively involved in reparative dentin formation (Figures S7L and S7M).

Incisor MSCs Are Typical MSCs In Vitro and Are All Derived from Gli1$^+$ Cells, but Not NG2$^+$ Cells

Next, we analyzed the incisor MSCs in vitro. Cells were obtained from the incisor mesenchyme and cultured under standard conditions. FACS analysis was performed on cultured postnatal day 0 (P0) or P1 cells. These cells strongly express typical MSC markers including CD105 (79%), CD146 (52%), Sca1 (80%), CD73 (93%), CD44 (88%), and nestin (90%) (Figure 6A). They are negative for CD34 (3.8%), CD45 (3.7%), CD130 (2.5%), and CD271 (2%). Under appropriate conditions, incisor mesenchymal cells were able to differentiate into calcified tissue (Figure 6B), adipose tissue (Figure 6C), and chondrocytes (Figures 6D and 6E). Therefore, based on their surface marker expression profile and trilineage differentiation ability, incisor MSCs can be considered typical MSCs.

Using cells derived from *Gli1-LacZ* mouse incisors, we determined that incisor MSCs lost Gli1 expression rapidly after migration out of the tissue block. This reduction is probably due to loss of the in vivo NVB niche. Therefore, to test the contribution of Gli1$^+$ cells to the MSCs in vitro, we induced *Gli1-CE;Tdtomato* mice. Mesenchymal cells harvested from the incisors of these mice were plated on a culture dish 72 hr after the first induction. Although only a small percentage of cells were labeled 72 hr after induction (Figure 2D), nearly all the cells (95%, n = 3) on the culture dish were positively labeled 10 days after plating, indicating that Gli1$^+$ cell derivatives ultimately populated the entire culture dish (Figures 6H–6J). Immunohistochemical staining indicated that all CD146$^+$, CD105$^+$, Sca1$^+$, and CD73$^+$ cells were derived from Gli1$^+$ cells (Figures 6K–6N).

For comparison, we also evaluated the contribution of NG2$^+$ cells to the MSCs in vitro. Cells were obtained from adult *NG2-Cre^{ER};ROSA26$^{LoxP\text{-}STOP\text{-}LoxP\text{-}Tdtomato}$* (*NG2-CE;Tdtomato*) mouse incisors 72 hr after induction. Although a few positive colonies could be detected 10 days after plating, NG2$^+$ cell derivatives only comprised a small percentage (<10%, n = 3) of the MSC population in the culture dish (Figures 6O and 6P). Therefore, in agreement with our in vivo experiments, our in vitro data demonstrate that periarterial Gli1$^+$ cells give rise to the entire MSC population in vitro and that NG2$^+$ pericytes only represent an MSC subpopulation.

DISCUSSION

Two fundamental questions in the study of MSCs are centered on where the MSC niche is located and what the bona fide identity of MSCs is in vivo. Using the mouse incisor as a model, our study provides definitive answers to both questions.

The perivasculature has been proposed to be the niche for various types of MSCs and many other stem cells (Crisan et al., 2008; Kokovay et al., 2010; Krautler et al., 2012; Tang et al., 2008). Nevertheless, it remains largely unknown how the vasculature regulates MSCs and whether arteries, veins, and capillaries comprise different MSC niches. A recent study suggested that CD34$^+$ periarterial adventitial cells may represent a different group of MSCs than the pericytes surrounding the capillaries and that cells obtained from the adventitia can differentiate into pericytes in vitro (Corselli et al., 2012). Our results indicate that the incisor MSCs are localized surrounding arterioles and are regulated by the NVB niche. They do not express typical MSC markers or CD34$^+$ and comprise less than 5% of the entire incisor mesenchyme. It is noteworthy that Gli1$^+$ cells or LRCs surround only arterioles accompanied by nerves, not all arterioles (see Figures 1C and 2C), consistent with an essential role for the nerve in the MSC niche.

The mouse incisor is innervated by sensory and sympathetic nerves (Ishizuka and Hiura, 1992; Johansson et al., 1992; Tabata et al., 1998; Zhang et al., 1998) but is devoid of parasympathetic nerves (Olgart, 1996; Sasano et al., 1995). Nerve fibers accompanying the arteries are located within the periarterial region, which is similar to the tunica adventitia of free arteries. These nerves are unmyelinated fibers surrounded by S100$^+$

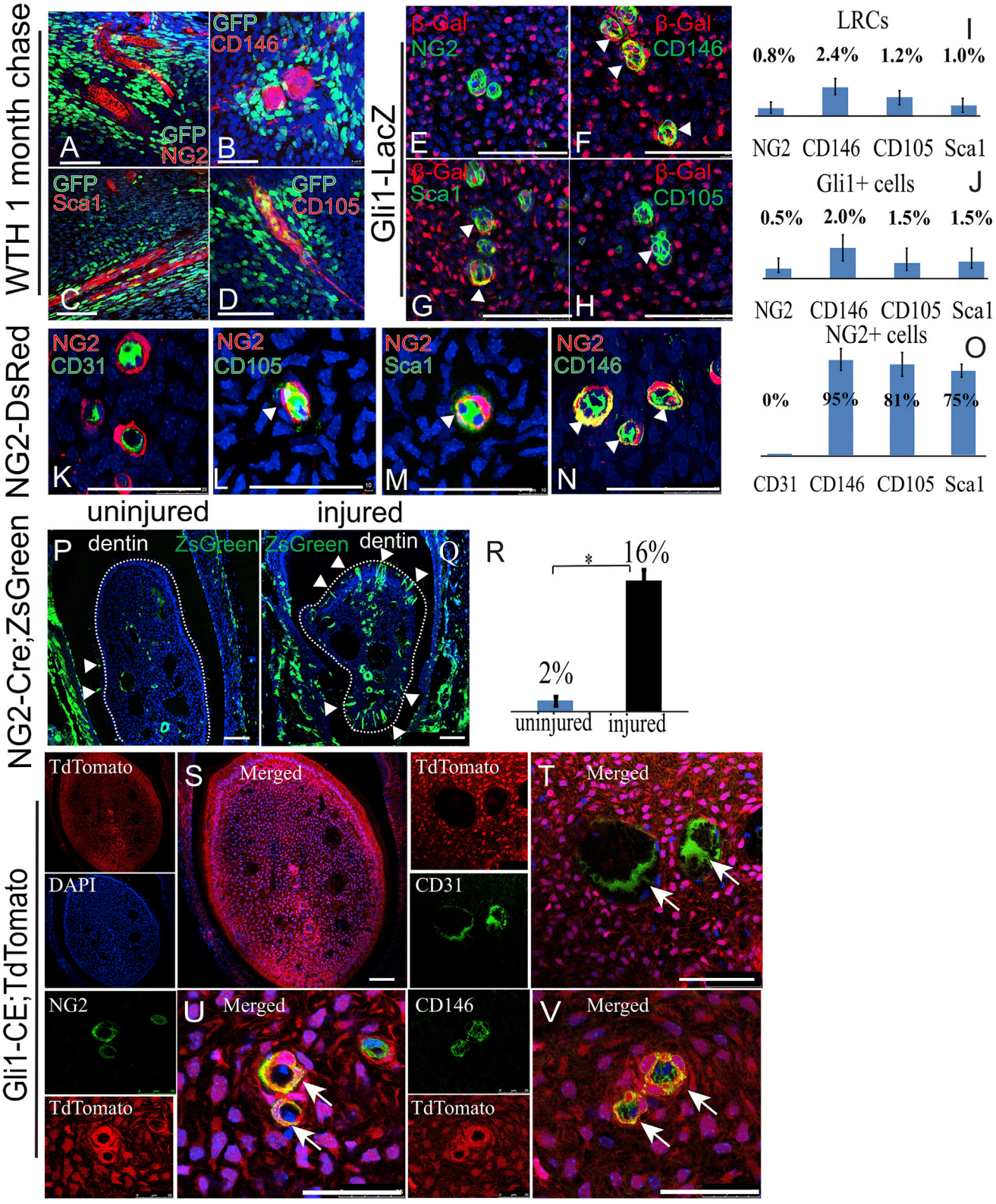

Figure 5. Gli1⁺ Cells Do Not Express Classical MSC Markers

NG2⁺ cells are pericytes derived from Gli1⁺ cells that express classical MSC markers and contribute mainly to injury repair, but not homeostasis.
(A–D) Immunohistochemical staining of CD146, CD105, Sca1, and NG2 (red) in chased adult *WTH* mouse incisors (LRCs appear green due to H2BGFP).

(legend continued on next page)

glial cells (Ishizuka and Hiura, 1992; Zhang et al., 1998). We show here that Shh produced by sensory neurons of the TGG is transported through the IAN and activates Gli1 expression in adjacent periarterial mesenchymal cells (Figure 7A). The hedgehog signaling pathway is critical for the commitment of the osteoblast lineage (Rodda and McMahon, 2006). In the incisor, it is possible that the Shh signal from the sensory nerve also regulates the odontogenic commitment of incisor MSCs. Crosstalk between sensory nerves and arteries regulates the formation of the NVB during development (Lawson et al., 2002; Li et al., 2013; Mukouyama et al., 2002, 2005). Our study indicates that this crosstalk continues into adulthood. Disruption of the NVB environment alters MSC homeostasis, as demonstrated by our denervation experiment. It remains unknown how artery components regulate the MSCs. Gli1$^+$ cells surrounding arteries have been observed throughout the body and have been proposed to be the stem cells for the arterial walls (Majesky et al., 2012; Passman et al., 2008). Although the NVB is a common anatomical structure throughout the body, it will require further study to determine whether the NVB also functions as an MSC niche in other organs. In a previous study, Shh regulating hair bulge stem cells was provided by CGRP$^-$;Runx3$^+$ proprioceptive sensory neurons of the dorsal root ganglion (DRG) (Brownell et al., 2011). In our study, Shh was provided by CGRP$^+$ neurons of the TGG. Such a difference might be due to the distinct developmental origins of the DRG and TGG and the lack of proprioceptive sensory neurons in the TGG (Senzaki et al., 2010). Shh from the dental epithelium has been proposed to regulate the differentiation of dental mesenchymal cells (Seidel et al., 2010). Although our data from *K14-rtTA;tetO-Cre;Shh$^{flox/flox}$* mice do not support this hypothesis, we do not rule out the possibility that Shh derived from dental epithelium may regulate the dental MSCs during embryonic development.

The NVB contains more than just nerves and arteries. Glial cells and endothelium may also play roles in the MSC niche. Intriguingly, our immunostaining and real-time PCR data showed that the number of glial cells and expression of myelination-related genes increased after denervation. In addition, Wnt signaling appeared to be inhibited after denervation. Wnt inhibition may be related to the reduced proliferation in the mesenchyme. None of these effects are clearly related to Shh signaling. Denervation not only interrupts the Shh signaling pathway but also many other signals, consistent with the extensive gene expression changes shown by our microarray results. In addition, the phenotypes in the incisor after denervation or Shh inhibitor administration are similar, but not identical. Although both procedures led to reduced dentin formation, the Shh inhibitor did not alter mesenchymal cell proliferation or stem cell maintenance, whereas denervation did. Therefore, Shh cannot be the only molecule secreted from the nerve that regulates MSCs. It remains unknown whether other factors, such as vascular endothelial growth factor, also regulate MSC function (Lawson et al., 2002; Mukouyama et al., 2002). It also remains unknown whether cellular components such as glial cells or endothelium participate in niche regulation. The NVB is an intricate environment composed of multiple molecular and cellular components, and it will require future studies to elucidate their contribution to the MSC niche.

Defining MSCs has been difficult and controversial. Although the definitions of most other stem cell types are based on their in vivo abilities to support homeostasis or injury repair (Grompe, 2012), the definition of MSCs currently relies mostly on unreliable in vitro assays and surface marker analysis. In addition, stem cells in other organs usually comprise a very small percentage of the entire population, but the MSC definition has included the majority of the cell population on the culture dish based on their high expression of classical MSC markers including CD73, CD105, Sca1, and others (Bianco et al., 2013; Covas et al., 2008; Crisan et al., 2008; Dominici et al., 2006; Traktuev et al., 2008).

Here, we identified Gli1 as an in vivo MSC marker that fulfills both the rigorous in vivo criteria established in many other stem cell studies and the in vitro criteria used in traditional MSC studies. Our results indicate that the classical MSC markers may not be appropriate markers to identify MSCs in vivo. In the incisor, these markers define pericytes that surround all vasculature in vivo, but the pericytes are derived from more primitive Gli1$^+$ MSCs that do not express these markers (see Figure 7B). The pericytes mainly function in injury repair, but not homeostasis. It is possible that the pericytes are a subpopulation of MSCs that participate in emergency responses such as injury repair and their intimate association with all vasculature enables them to respond immediately to tissue injury. These observations also suggest that injury

(E–H) Coimmunohistochemical staining of β-gal (red) with MSC markers (green) NG2, CD146, Sca1, and CD105 in *Gli1-LacZ* mouse incisors at 1 month of age. Colocalization appears yellow, indicated by arrowheads.
(I and J) Quantification of results from (A)–(H) indicates that the majority of LRCs and Gli1$^+$ cells are negative for MSC markers. Values are plotted as mean ± SEM.
(K–N) Immunohistochemical staining of CD31 and MSC markers (green) including CD105, Sca1, and CD146 in the incisor mesenchyme of *NG2-DsRed* mice. Yellow indicates coexpression (arrowheads). DAPI is in blue.
(O) Quantification of results from (K)–(N) indicates that NG$^+$ cells are pericytes expressing MSC markers. Values are plotted as mean ± SEM.
(P and Q) NG2-derived cells (green) in the incisor mesenchyme of *NG2-Cre;ZsGreen* mice untreated (P) or 3 weeks after injury (Q) (n = 6). Arrowheads indicate odontoblasts derived from NG2$^+$ cells. Dotted line outlines pulp chamber.
(R) Quantification of the percentage of NG2 derived odontoblasts from (P) and (Q). Values are plotted as mean ± SEM (*$p < 0.05$, n = 6). S. Single and merged staining of cross section of *Gli-CE;TdTomato* incisor 1 month after tamoxifen induction. TdTomato fluorescence (red) marks cells derived from Gli1$^+$ cells. DAPI is blue.
(T) Endothelium marker CD31 (green) immunostaining of incisors from *Gli-CE;TdTomato* mice 1 month after tamoxifen induction. Arrows indicate CD31$^+$ endothelium is not derived from Gli1$^+$ cells.
(U and V) Immunohistochemical staining (green) of NG2 (U) and CD146 (V) in *Gli-CE;TdTomato* mouse incisor 1 month after induction indicates that NG2$^+$ and CD146$^+$ cells are derived from Gli1$^+$ cells. Colocalization appears yellow, indicated with arrows.
Scale bars, 100 μm.

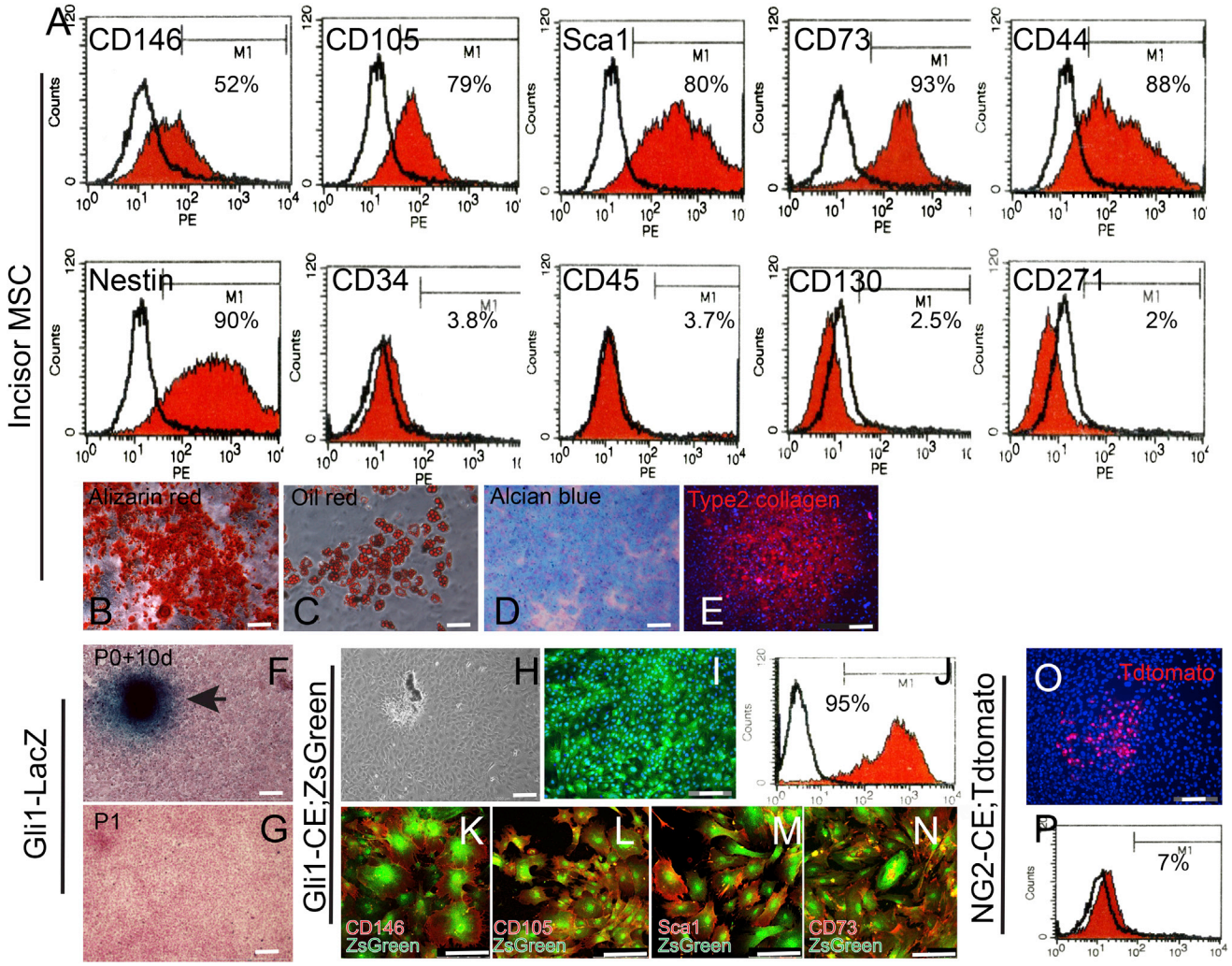

Figure 6. Incisor MSCs Derived from Gli1$^+$ Cells Are Typical MSCs In Vitro

(A) FACS analysis of cells obtained from cultured incisor mesenchymal cells indicates they strongly express CD146, CD105, Sca1, CD73, CD44, and nestin but are negative for CD34, CD45, CD130, and CD271.

(B) Alizarin red staining of cultured incisor mesenchymal cells 2 weeks after osteogenic induction.

(C) Oil red staining of cultured incisor mesenchymal cells 2 weeks after adipogenic induction.

(D and E) Alcian blue staining (D) and type II collagen staining (E) of incisor mesenchymal cells 1 month after chondrogenic induction.

(F and G) LacZ staining of cultured cells obtained from *Gli1-LacZ* mouse incisors at 10 days after plating (F) or at P1 (G). Cells were counterstained with nuclear fast red.

(H–J) Phase contrast (H) and fluorescent images (I) of cultured incisor mesenchymal cells from adult *Gli1-CE;ZsGreen* mice. Cultures were analyzed 10 days after plating. ZsGreen fluorescence indicates cells derived from Gli1$^+$ cells. FACS analysis indicates that approximately 95% of cells on the culture dish are derived from Gli1$^+$ cells (J).

(K–N) Immunohistochemical staining of MSC markers CD146, CD105, Sca1, and CD73 (red) in cultured incisor mesenchymal cells from adult *Gli1-CE;ZsGreen* mice. Cells expressing these MSC markers are all derived Gli1$^+$ cells.

(O and P) Cultured incisor mesenchymal cells from *NG2-CE;TdTomato* mouse incisors 72 hr after induction. Cultures were analyzed 10 days after plating. TdTomato fluorescence indicates cells derived from NG2$^+$ cells (O). FACS analysis indicates that approximately 7% of cells on the culture dish are derived from NG2$^+$ cells (P).

repair should be considered distinct from physiological homeostasis. These processes might be regulated by different activation mechanisms and supported by different stem cell populations. Interestingly, the differential contribution of stem cells to homeostasis and repair has also been shown in the hair follicle (Ito et al., 2005). This difference may also raise questions as to the utility of evaluating stem cell properties with transplantation assays, because transplantation is more similar to injury repair than to homeostasis and is not a physiological process.

Our study also highlights the incisor as an excellent model for studying MSCs. The significance of the mouse incisor as a stem cell model has long been overlooked, likely because continuously growing incisors are unique to rodents and adult human

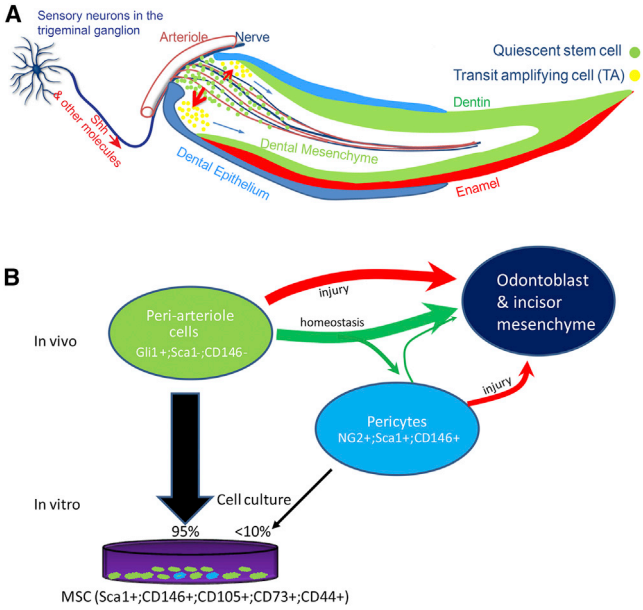

Figure 7. Schematic Diagram of Our Model of the NVB Niche and the In Vivo Origin of Incisor MSCs

(A) The NVB provides a niche to support the continuous turnover of incisor mesenchyme. Sensory neurons in the trigeminal ganglion produce Shh, which is transported through axons into the incisor mesenchyme. Shh activates Gli1 expression in the quiescent stem cells surrounding the arterioles near the cervical loop region and regulates the odontogenic differentiation process. These quiescent stem cells continuously give rise to actively dividing TACs, which then differentiate into odontoblasts and all other dental mesenchymal derivatives to support the rapid cellular turnover of the incisor.

(B) In vivo origin of the incisor MSCs. The $Gli1^+$ cells surrounding the NVB are the most primitive MSC population. They continuously give rise to odontoblasts under both homeostasis and injury-repair situations. The majority of $Gli1^+$ cells do not express classical MSC markers including CD146, CD105, and Sca1. $NG2^+$ cells are pericytes surrounding all vasculature and express classical MSC markers. $NG2^+$ cells are an MSC subpopulation derived from $Gli1^+$ cells. They mainly function in injury repair, but not in homeostasis. Incisor MSCs on the culture dish are entirely derived from periarterial $Gli1^+$ cells, but only a few are derived from $NG2^+$ cells. In summary, incisor MSCs originate from periarterial cells in vivo and are supported by the NVB niche.

teeth do not grow continuously. With the establishment of Gli1 as an in vivo marker, we will be able to target MSCs specifically and precisely to inactivate a specific gene in order to test its in vivo function in regulating MSCs.

In summary, our study identifies an unexpected function for the neurovascular bundle, as an MSC niche, and clarifies the identity and functions of MSCs in vivo (Figures 7A and 7B). Using the incisor as a model, we show that MSCs originate from periarterial cells in vivo and are supported by the NVB niche. These periarterial cells support incisor homeostasis and give rise to the entire MSC population in vitro. In contrast, conventional MSC surface markers define pericytes that make only a minor contribution to incisor homeostasis in vivo or to the MSC population in vitro. These pericytes contribute mainly to injury repair, but not to homeostasis. Collectively, our discoveries will have an important impact on the definition and identification of MSCs in vivo.

EXPERIMENTAL PROCEDURES

Animals and Tamoxifen Administration

All animal models (16 different transgenic lines), their source of origin (e.g., Jackson Laboratory ID#), and original references describing each of these 16 transgenic lines are listed in Table S1. All mouse experiments were conducted in accordance with protocols approved by the Department of Animal Resources and the Institutional Animal Care and Use Committee of the University of Southern California. Tamoxifen (Sigma) was dissolved in corn oil (20 mg/ml) and injected intraperitoneally (i.p.; 10 mg daily for 3 days). EdU (200 mg/kg) was injected i.p. 2 hr prior to sacrifice.

X-gal Staining

Samples from mice were fixed in 0.2% glutaraldehyde and decalcified with 20% EDTA for 2 weeks. Frozen sections of 12 μm thickness were cut prior to X-gal staining. Detection of β-gal activity in tissue sections was carried out as per standard protocol.

Immunofluorescent Staining and In Situ Hybridization

The following antibodies were used in our study: αSMA (Abcam ab5694 1:100), β3-tubulin (Abcam ab78078, 1:1,000), S100b (Abcam ab868, 1:1000), Shh (Abcam ab73958, 1:100), nestin (Abcam ab6142, 1:200), Th (Abcam ab6211, 1:1,000), CGRP (Abcam ab4901, 1:1,000), CD31 (BD Bioscience 550274, 1:25), β-gal (MP Biomedical NBP1-78259, 1:50), Gli1 (Novus Biological NBP1-78259, 1:25), NG2 (Millipore MAB5384, 1:200), CD146 (BD Biosciences 562230, 1:100), CD105 (BD Biosciences 555690, 1:100), Sca1 (BD Biosciences 558162, 1:100), PDGFrβ (eBiosciences 14-1402-82, 1:100), CD44 (BD Biosciences 553134, 1:100), CD130 (BD Biosciences 555757, 1:100), GFP (Abcam ab1218, 1:100), and BrdU (Invitrogen 93-3944, ready to use). Staining was performed according to standard procedures. Shh exon2 probe was kindly provided by Andrew McMahon (Dassule et al., 2000). In situ hybridization was performed according to standard procedures.

Injury Assay

The incisor injury protocol was adapted from a previous study (Feng et al., 2011). For the molar injury assay, molars were drilled with size 25 endodontic files to expose the pulp cavity and then covered with dental cement. For vasculature injury, a 28G needle was used to puncture through the mandibular foramen to damage the inferior alveolar artery.

Denervation Surgery

The inferior alveolar nerve was severed using microsurgery as previously described (Chiego et al., 1981). A sham operation was performed on the other side of the same animal following the same surgical procedures except for resection of the nerve to create a control. The denervation procedure had no impact on food or water uptake or the general health condition of the mice.

Label-Resisting Analysis

Six- to 12-week-old guinea pigs were given i.p. injections of BrdU (150 mg/kg) for 10 consecutive days. Samples were collected 2 hr after the last injection and processed for further analysis.

Incisor Mesenchymal Cell Culture and Differentiation

Incisor pulp was obtained from mouse lower incisors and the dental epithelium was carefully removed with fine forceps. The pulp tissue was minced into 0.5 mm pieces and the tissue blocks were transferred into a T25 culture flask (Corning) and incubated with αMEM + 20% fetal bovine serum (GIBCO) containing ascorbic acid and glutamate (Gibco) at 37°C in 5% CO_2. Osteogenic, adipogenic, or chondrogenic differentiation was performed as previously described (Chung et al., 2009).

Statistical Analysis

SPSS13.0 was used for statistical analysis. Significance was assessed by independent two-tailed Student's t test or analysis of variance. $p < 0.05$ was considered statistically significant.

ACCESSION NUMBERS

The microarray data reported in this paper have been deposited in the National Center for Biotechnology Information Gene Expression Omnibus (http://www.ncbi.nih.gov/geo/) under series accession number GSE51479.

SUPPLEMENTAL INFORMATION

Supplemental Information for this article includes Supplemental Experimental Procedures, seven figures, and one table and can be found with this article online at http://dx.doi.org/10.1016/j.stem.2013.12.013.

AUTHOR CONTRIBUTIONS

H.Z. and Y.C. designed the study; H.Z. carried out the experiments and analyzed the data; J.F. participated in the guinea pig and microarray experiments; K.S. and O.K. did the cell lineage tracing and hedgehog inhibitor experiments; S.S. and P.S. contributed to the stem cell marker study; and H.Z. and Y.C. cowrote the paper.

ACKNOWLEDGMENTS

We thank Julie Mayo and Bridget Samuels for critical reading of the manuscript, Dr. Alexandra Joyner (Memorial Sloan-Kettering Cancer Center) for providing the Gli1-GFP mice, and Dr. Richard Pelikan for performing microarray analysis. H.Z. gratefully acknowledges training grant support from the National Institute of Dental and Craniofacial Research, National Insitutes of Health (R90 DE022528). P.S. acknowledges support from the Medical Research Council. This study was supported by grants from the National Institute of Dental and Craniofacial Research, National Insitutes of Health (DE022503, DE020065, and DE012711 to Y.C.).

Received: March 19, 2013
Revised: July 24, 2013
Accepted: December 19, 2013
Published: February 6, 2014

REFERENCES

Bai, C.B., Auerbach, W., Lee, J.S., Stephen, D., and Joyner, A.L. (2002). Gli2, but not Gli1, is required for initial Shh signaling and ectopic activation of the Shh pathway. Development *129*, 4753–4761.

Balic, A., and Mina, M. (2010). Characterization of progenitor cells in pulps of murine incisors. J. Dent. Res. *89*, 1287–1292.

Bernardo, M.E., and Fibbe, W.E. (2013). Mesenchymal stromal cells: sensors and switchers of inflammation. Cell Stem Cell *13*, 392–402.

Bianco, P., Robey, P.G., and Simmons, P.J. (2008). Mesenchymal stem cells: revisiting history, concepts, and assays. Cell Stem Cell *2*, 313–319.

Bianco, P., Cao, X., Frenette, P.S., Mao, J.J., Robey, P.G., Simmons, P.J., and Wang, C.Y. (2013). The meaning, the sense and the significance: translating the science of mesenchymal stem cells into medicine. Nat. Med. *19*, 35–42.

Brownell, I., Guevara, E., Bai, C.B., Loomis, C.A., and Joyner, A.L. (2011). Nerve-derived sonic hedgehog defines a niche for hair follicle stem cells capable of becoming epidermal stem cells. Cell Stem Cell *8*, 552–565.

Chan-Ling, T., and Hughes, S. (2005). NG2 can be used to identify arteries versus veins enabling the characterization of the different functional roles of arterioles and venules during microvascular network growth and remodeling. Microcirculation *12*, 539–540, author reply 540-531.

Chen, Z.L., Yu, W.M., and Strickland, S. (2007). Peripheral regeneration. Annu. Rev. Neurosci. *30*, 209–233.

Chiego, D.J., Jr., Klein, R.M., and Avery, J.K. (1981). Tritiated thymidine autoradiographic study of the effects of inferior alveolar nerve resection on the proliferative compartments of the mouse incisor formative tissues. Arch. Oral Biol. *26*, 83–89.

Chiego, D.J., Jr., Fisher, M.A., Avery, J.K., and Klein, R.M. (1983). Effects of denervation on 3H-fucose incorporation by odontoblasts in the mouse incisor. Cell Tissue Res. *230*, 197–203.

Chung, I.H., Yamaza, T., Zhao, H., Choung, P.H., Shi, S., and Chai, Y. (2009). Stem cell property of postmigratory cranial neural crest cells and their utility in alveolar bone regeneration and tooth development. Stem Cells *27*, 866–877.

Corselli, M., Chen, C.W., Sun, B., Yap, S., Rubin, J.P., and Péault, B. (2012). The tunica adventitia of human arteries and veins as a source of mesenchymal stem cells. Stem Cells Dev. *21*, 1299–1308.

Covas, D.T., Panepucci, R.A., Fontes, A.M., Silva, W.A., Jr., Orellana, M.D., Freitas, M.C., Neder, L., Santos, A.R., Peres, L.C., Jamur, M.C., and Zago, M.A. (2008). Multipotent mesenchymal stromal cells obtained from diverse human tissues share functional properties and gene-expression profile with CD146+ perivascular cells and fibroblasts. Exp. Hematol. *36*, 642–654.

Crisan, M., Yap, S., Casteilla, L., Chen, C.W., Corselli, M., Park, T.S., Andriolo, G., Sun, B., Zheng, B., Zhang, L., et al. (2008). A perivascular origin for mesenchymal stem cells in multiple human organs. Cell Stem Cell *3*, 301–313.

Dassule, H.R., Lewis, P., Bei, M., Maas, R., and McMahon, A.P. (2000). Sonic hedgehog regulates growth and morphogenesis of the tooth. Development *127*, 4775–4785.

Dellavalle, A., Maroli, G., Covarello, D., Azzoni, E., Innocenzi, A., Perani, L., Antonini, S., Sambasivan, R., Brunelli, S., Tajbakhsh, S., and Cossu, G. (2011). Pericytes resident in postnatal skeletal muscle differentiate into muscle fibres and generate satellite cells. Nat. Commun. *2*, 499.

Dominici, M., Le Blanc, K., Mueller, I., Slaper-Cortenbach, I., Marini, F., Krause, D., Deans, R., Keating, A., Prockop, Dj., and Horwitz, E. (2006). Minimal criteria for defining multipotent mesenchymal stromal cells. The International Society for Cellular Therapy position statement. Cytotherapy *8*, 315–317.

Feng, J., Mantesso, A., De Bari, C., Nishiyama, A., and Sharpe, P.T. (2011). Dual origin of mesenchymal stem cells contributing to organ growth and repair. Proc. Natl. Acad. Sci. USA *108*, 6503–6508.

Fitch, S.R., Kimber, G.M., Wilson, N.K., Parker, A., Mirshekar-Syahkal, B., Göttgens, B., Medvinsky, A., Dzierzak, E., and Ottersbach, K. (2012). Signaling from the sympathetic nervous system regulates hematopoietic stem cell emergence during embryogenesis. Cell Stem Cell *11*, 554–566.

Foudi, A., Hochedlinger, K., Van Buren, D., Schindler, J.W., Jaenisch, R., Carey, V., and Hock, H. (2009). Analysis of histone 2B-GFP retention reveals slowly cycling hematopoietic stem cells. Nat. Biotechnol. *27*, 84–90.

Friedenstein, A.J., Petrakova, K.V., Kurolesova, A.I., and Frolova, G.P. (1968). Heterotopic of bone marrow. Analysis of precursor cells for osteogenic and hematopoietic tissues. Transplantation *6*, 230–247.

Grompe, M. (2012). Tissue stem cells: new tools and functional diversity. Cell Stem Cell *10*, 685–689.

Harada, H., Kettunen, P., Jung, H.S., Mustonen, T., Wang, Y.A., and Thesleff, I. (1999). Localization of putative stem cells in dental epithelium and their association with Notch and FGF signaling. J. Cell Biol. *147*, 105–120.

Hashimoto, E., Nakakura-Ohshima, K., Kenmotsu, S., Suzuki, H., Nakasone, N., Saito, C., Harada, H., and Ohshima, H. (2008). The relationship between the cusp pattern and plural stem cell compartments in Guinea pig cheek teeth by chasing BrdU-labeling. Arch. Histol. Cytol. *71*, 317–332.

Ishizuka, H., and Hiura, A. (1992). A light and electron microscopic study on pulpal nerve fibers in the lower incisor of the mouse. Arch. Histol. Cytol. *55*, 167–178.

Ito, M., Liu, Y., Yang, Z., Nguyen, J., Liang, F., Morris, R.J., and Cotsarelis, G. (2005). Stem cells in the hair follicle bulge contribute to wound repair but not to homeostasis of the epidermis. Nat. Med. *11*, 1351–1354.

Jiang, J., and Hui, C.C. (2008). Hedgehog signaling in development and cancer. Dev. Cell *15*, 801–812.

Johansson, C.S., Hildebrand, C., and Povlsen, B. (1992). Anatomy and developmental chronology of the rat inferior alveolar nerve. Anat. Rec. *234*, 144–152.

Juuri, E., Saito, K., Ahtiainen, L., Seidel, K., Tummers, M., Hochedlinger, K., Klein, O.D., Thesleff, I., and Michon, F. (2012). Sox2+ stem cells contribute

to all epithelial lineages of the tooth via Sfrp5+ progenitors. Dev. Cell *23*, 317–328.

Katayama, Y., Battista, M., Kao, W.M., Hidalgo, A., Peired, A.J., Thomas, S.A., and Frenette, P.S. (2006). Signals from the sympathetic nervous system regulate hematopoietic stem cell egress from bone marrow. Cell *124*, 407–421.

Keating, A. (2012). Mesenchymal stromal cells: new directions. Cell Stem Cell *10*, 709–716.

Kerezoudis, N.P., Fried, K., and Olgart, L. (1995). Haemodynamic and immunohistochemical studies of rat incisor pulp after denervation and subsequent re-innervation. Arch. Oral Biol. *40*, 815–823.

Knox, S.M., Lombaert, I.M., Reed, X., Vitale-Cross, L., Gutkind, J.S., and Hoffman, M.P. (2010). Parasympathetic innervation maintains epithelial progenitor cells during salivary organogenesis. Science *329*, 1645–1647.

Knox, S.M., Lombaert, I.M., Haddox, C.L., Abrams, S.R., Cotrim, A., Wilson, A.J., and Hoffman, M.P. (2013). Parasympathetic stimulation improves epithelial organ regeneration. Nat. Commun. *4*, 1494.

Kokovay, E., Goderie, S., Wang, Y., Lotz, S., Lin, G., Sun, Y., Roysam, B., Shen, Q., and Temple, S. (2010). Adult SVZ lineage cells home to and leave the vascular niche via differential responses to SDF1/CXCR4 signaling. Cell Stem Cell *7*, 163–173.

Krautler, N.J., Kana, V., Kranich, J., Tian, Y., Perera, D., Lemm, D., Schwarz, P., Armulik, A., Browning, J.L., Tallquist, M., et al. (2012). Follicular dendritic cells emerge from ubiquitous perivascular precursors. Cell *150*, 194–206.

Kubota, K., Yonaga, T., Hosaka, K., Katayama, T., Nagae, K., Shibanai, S., Sato, Y., and Takada, K. (1985). Experimental morphological studies on the functional role of the pulpal nerves in dentinogenesis. Anat. Anz. *158*, 323–336.

Ladizesky, M.G., Lama, M.A., Cutrera, R.A., Boggio, V., Giglio, M.J., and Cardinali, D.P. (2001). Effect of unilateral superior cervical ganglionectomy on mandibular incisor eruption rate in rats. Auton. Neurosci. *93*, 65–70.

Lapthanasupkul, P., Feng, J., Mantesso, A., Takada-Horisawa, Y., Vidal, M., Koseki, H., Wang, L., An, Z., Miletich, I., and Sharpe, P.T. (2012). Ring1a/b polycomb proteins regulate the mesenchymal stem cell niche in continuously growing incisors. Dev. Biol. *367*, 140–153.

Lawson, N.D., Vogel, A.M., and Weinstein, B.M. (2002). sonic hedgehog and vascular endothelial growth factor act upstream of the Notch pathway during arterial endothelial differentiation. Dev. Cell *3*, 127–136.

Li, W., Kohara, H., Uchida, Y., James, J.M., Soneji, K., Cronshaw, D.G., Zou, Y.R., Nagasawa, T., and Mukouyama, Y.S. (2013). Peripheral nerve-derived CXCL12 and VEGF-A regulate the patterning of arterial vessel branching in developing limb skin. Dev. Cell *24*, 359–371.

Majesky, M.W., Dong, X.R., Hoglund, V., Daum, G., and Mahoney, W.M., Jr. (2012). The adventitia: a progenitor cell niche for the vessel wall. Cells Tissues Organs *195*, 73–81.

Mao, J.J., and Prockop, D.J. (2012). Stem cells in the face: tooth regeneration and beyond. Cell Stem Cell *11*, 291–301.

Méndez-Ferrer, S., Michurina, T.V., Ferraro, F., Mazloom, A.R., Macarthur, B.D., Lira, S.A., Scadden, D.T., Ma'ayan, A., Enikolopov, G.N., and Frenette, P.S. (2010). Mesenchymal and haematopoietic stem cells form a unique bone marrow niche. Nature *466*, 829–834.

Miura, M., Gronthos, S., Zhao, M., Lu, B., Fisher, L.W., Robey, P.G., and Shi, S. (2003). SHED: stem cells from human exfoliated deciduous teeth. Proc. Natl. Acad. Sci. USA *100*, 5807–5812.

Mukouyama, Y.S., Shin, D., Britsch, S., Taniguchi, M., and Anderson, D.J. (2002). Sensory nerves determine the pattern of arterial differentiation and blood vessel branching in the skin. Cell *109*, 693–705.

Mukouyama, Y.S., Gerber, H.P., Ferrara, N., Gu, C., and Anderson, D.J. (2005). Peripheral nerve-derived VEGF promotes arterial differentiation via neuropilin 1-mediated positive feedback. Development *132*, 941–952.

Murfee, W.L., Skalak, T.C., and Peirce, S.M. (2005). Differential arterial/venous expression of NG2 proteoglycan in perivascular cells along microvessels: identifying a venule-specific phenotype. Microcirculation *12*, 151–160.

Olgart, L. (1996). Neural control of pulpal blood flow. Crit. Rev. Oral Biol. Med. *7*, 159–171.

Parsa, S., Kuremoto, K., Seidel, K., Tabatabai, R., Mackenzie, B., Yamaza, T., Akiyama, K., Branch, J., Koh, C.J., Al Alam, D., et al. (2010). Signaling by FGFR2b controls the regenerative capacity of adult mouse incisors. Development *137*, 3743–3752.

Passman, J.N., Dong, X.R., Wu, S.P., Maguire, C.T., Hogan, K.A., Bautch, V.L., and Majesky, M.W. (2008). A sonic hedgehog signaling domain in the arterial adventitia supports resident Sca1+ smooth muscle progenitor cells. Proc. Natl. Acad. Sci. USA *105*, 9349–9354.

Pittenger, M.F., Mackay, A.M., Beck, S.C., Jaiswal, R.K., Douglas, R., Mosca, J.D., Moorman, M.A., Simonetti, D.W., Craig, S., and Marshak, D.R. (1999). Multilineage potential of adult human mesenchymal stem cells. Science *284*, 143–147.

Rodda, S.J., and McMahon, A.P. (2006). Distinct roles for Hedgehog and canonical Wnt signaling in specification, differentiation and maintenance of osteoblast progenitors. Development *133*, 3231–3244.

Sasano, T., Shoji, N., Kuriwada, S., Sanjo, D., Izumi, H., and Karita, K. (1995). Absence of parasympathetic vasodilatation in cat dental pulp. J. Dent. Res. *74*, 1665–1670.

Savastano, L.E., Castro, A.E., Fitt, M.R., Rath, M.F., Romeo, H.E., and Muñoz, E.M. (2010). A standardized surgical technique for rat superior cervical ganglionectomy. J. Neurosci. Methods *192*, 22–33.

Schwab, K.E., and Gargett, C.E. (2007). Co-expression of two perivascular cell markers isolates mesenchymal stem-like cells from human endometrium. Hum. Reprod. *22*, 2903–2911.

Seidel, K., Ahn, C.P., Lyons, D., Nee, A., Ting, K., Brownell, I., Cao, T., Carano, R.A., Curran, T., Schober, M., et al. (2010). Hedgehog signaling regulates the generation of ameloblast progenitors in the continuously growing mouse incisor. Development *137*, 3753–3761.

Senzaki, K., Ozaki, S., Yoshikawa, M., Ito, Y., and Shiga, T. (2010). Runx3 is required for the specification of TrkC-expressing mechanoreceptive trigeminal ganglion neurons. Mol. Cell. Neurosci. *43*, 296–307.

Smith, C.E., and Warshawsky, H. (1975). Cellular renewal in the enamel organ and the odontoblast layer of the rat incisor as followed by radioautography using 3H-thymidine. Anat. Rec. *183*, 523–561.

Tabata, S., Ozaki, H.S., Nakashima, M., Uemura, M., and Iwamoto, H. (1998). Innervation of blood vessels in the rat incisor pulp: a scanning electron microscopic and immunoelectron microscopic study. Anat. Rec. *251*, 384–391.

Tang, W., Zeve, D., Suh, J.M., Bosnakovski, D., Kyba, M., Hammer, R.E., Tallquist, M.D., and Graff, J.M. (2008). White fat progenitor cells reside in the adipose vasculature. Science *322*, 583–586.

Traktuev, D.O., Merfeld-Clauss, S., Li, J., Kolonin, M., Arap, W., Pasqualini, R., Johnstone, B.H., and March, K.L. (2008). A population of multipotent CD34-positive adipose stromal cells share pericyte and mesenchymal surface markers, reside in a periendothelial location, and stabilize endothelial networks. Circ. Res. *102*, 77–85.

Tumbar, T., Guasch, G., Greco, V., Blanpain, C., Lowry, W.E., Rendl, M., and Fuchs, E. (2004). Defining the epithelial stem cell niche in skin. Science *303*, 359–363.

Zhang, J.Q., Nagata, K., and Iijima, T. (1998). Scanning electron microscopy and immunohistochemical observations of the vascular nerve plexuses in the dental pulp of rat incisor. Anat. Rec. *251*, 214–220.

Zhu, X., Bergles, D.E., and Nishiyama, A. (2008). NG2 cells generate both oligodendrocytes and gray matter astrocytes. Development *135*, 145–157.

Zuk, P.A., Zhu, M., Ashjian, P., De Ugarte, D.A., Huang, J.I., Mizuno, H., Alfonso, Z.C., Fraser, J.K., Benhaim, P., and Hedrick, M.H. (2002). Human adipose tissue is a source of multipotent stem cells. Mol. Biol. Cell *13*, 4279–4295.